The particle valve: On-demand particle trapping, filtering, and release from a microfabricated polydimethylsiloxane membrane using surface acoustic waves

David J. Collins, Tuncay Alan, and Adrian Neild

Citation: Applied Physics Letters **105**, 033509 (2014); doi: 10.1063/1.4891424
View online: http://dx.doi.org/10.1063/1.4891424
View Table of Contents: http://scitation.aip.org/content/aip/journal/apl/105/3?ver=pdfcov
Published by the AIP Publishing

The particle valve: On-demand particle trapping, filtering, and release from a microfabricated polydimethylsiloxane membrane using surface acoustic waves

David J. Collins, Tuncay Alan, and Adrian Neild[a)]
Laboratory for Microsystems, Department of Mechanical and Aerospace Engineering, Monash University, Clayton, VIC 3800, Australia

(Received 4 April 2014; accepted 7 July 2014; published online 24 July 2014)

We introduce a surface acoustic wave (SAW) based method for acoustically controlled concentration, capture, release, and sorting of particles in a microfluidic system. This method is power efficient by the nature of its design: the vertical direction of a traveling acoustic wave, in which the majority of the energy at the SAW-water interface is directed, is used to concentrate particles behind a microfabricated polydimethylsiloxane membrane extending partially into a channel. Sorting is also demonstrated with this concentration shown to be size-dependent. Low-power, miniature SAW devices, using methods such as the one demonstrated here, are well placed for future integration into point-of-care diagnostic systems. © *2014 AIP Publishing LLC*.
[http://dx.doi.org/10.1063/1.4891424]

The separation, concentration, and general manipulation of particles and cells are vital functions for many microfluidic systems, where particles serve as surrogates for cells and large biomolecules, but also as therapeutic or diagnostic agents in their own right. With the increasing complexity and digital nature of advanced microfluidic systems, gating functions that control particle and cell movement are becoming increasingly important. Strategies for controlled particle trapping and release include mechanical,[1,2] optical,[3,4] hydrodynamic,[5] magnetic,[6,7] and acoustic methods.[8–10] Acoustic forces are well suited to the task, being non-contact and applicable to a wide range of particle and cell sizes and types, though have not been used extensively for on-chip gating and valves. This is due to lack of suitable geometries, release strategies, fabrication difficulties, and small acoustic force gradients on the scale of a micron-sized particles, especially if lower frequencies ($\lesssim$5 MHz) with relatively large wavelengths ($\gtrsim$500 μm) are used. However, surface acoustic waves (SAWs), with typical wavelengths (4–300 μm) on the order of length scales of microfluidic systems, are well suited to biological assays where items on the scale of cells are manipulated.

To date, the vast majority of applications using SAW exploit the forces in the horizontal plane.[8,11–17] It may, however, be more sensible in some cases to take advantage of the force component in the vertical direction, considering that the major component of the traveling wave force is directed vertically. Due to the value of the Rayleigh angle θ_R, which describes the orientation of the acoustic force relative to the solid/fluid interface, the horizontal force is only a fraction of the vertical one. Despite this, there have been only select cases to date that explicitly utilize this as their mode of operation in closed microfluidic systems. The limiting factor in making use of the vertical force in closed systems, however, is a result of fabrication difficulties. Dentry *et al.*[18] used a 3D fabricated chamber to optimize the pumping force generated using SAW, with a pumping chamber angled at θ_R. In the future, though, 3D printed microfluidic devices will require further optimization and development to integrate with SAW devices to match the device quality and spatial resolution of conventional fabrication techniques.

In this work, we demonstrate the first explicit use of the vertical component of traveling SAW to trap and concentrate particles and release them on-demand. The proposed method makes use of a topographical polydimethylsiloxane (PDMS) feature easily constructed with standard microfabrication techniques and without the need for multilayer processes. By actively trapping and passively releasing particles, we show that it is possible to use this method to both control the timing of particle concentration and also filter them by size, all while making efficient use of the vertical orientation of an acoustic wave generated by SAW. Furthermore, the procedure used to fabricate this 3D structure in PDMS does not require gray-scale lithography, relying instead on the intrinsic changes in etch rates during deep reactive-ion etching (DRIE) when the movement of reactive ions is impeded in a high-aspect ratio feature. It is thought that this method for fabricating simple vertically varying features will find use in other applications where thin quasi-3D PDMS structures, including membranes, rods, and flaps, are required.

When an acoustic wave traveling through a fluid medium encounters an object with non-zero acoustic contrast, that object will be subjected to a time-averaged force.[19] For a particle in an acoustic field, this force is fundamentally due to the interference between the scattered field that it creates and the incident acoustic beam,[20,21] and is always oriented in the direction of the traveling wave acoustic beam.[22] In the case of a traveling substrate-bound wave, such as SAW, these surface displacements will couple into a fluid placed on top of the substrate, with the resulting beam propagating at the Rayleigh angle, given by $\theta_R = \sin^{-1}(c_f/c_s)$, where c_f and c_s are the sound speed in the fluid and the SAW velocity of the substrate. For water and lithium niobate (LN), a piezoelectric material commonly used for SAW applications, this angle is $\approx$22° from the vertical, with the relative magnitude of the vertical to the horizontal components given by

a)Electronic mail: Adrian.Neild@monash.edu

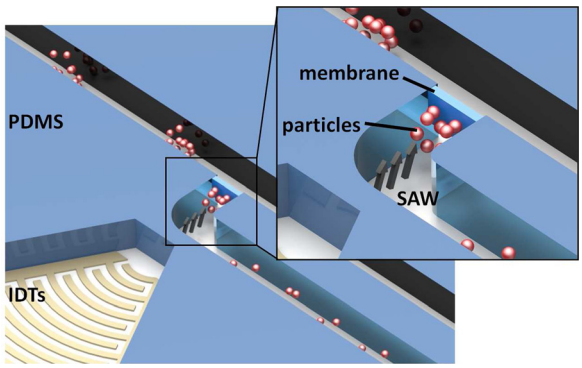

FIG. 1. Controlled release concept: a SAW generated by a series of focussed IDTs on a piezoelectric substrate generates an acoustic field that imparts a force, mostly in the vertical direction, against particles in a fluid flow. Without SAW applied, particles pass through the gap under the membrane unimpeded. However, subject to this force, particles are unable to pass beyond a microfabricated PDMS membrane in their path. This methodology enables on-demand particle concentration and release.

$\cos(22°)/\sin(22°)$; the vertical force is therefore approximately 2.5 times that of the horizontal one.

Figure 1 shows the system concept: a particle solution is injected perpendicular to a continuous flow channel in a T-junction configuration, with particle concentration and controlled release mediated by the application of SAW. Figure 2 shows this process in more detail, especially, with regard to the critical role of a PDMS membrane, which partially protrudes into the channel from which the particles originate. Provided the gap between the channel floor and the bottom of the membrane is sufficiently large, particles pass unimpeded in the direction of fluid flow. With the application of SAW, a traveling wave force is imparted on the particles in suspension, where after they are pushed both against the channel roof and the PDMS membrane.

The SAW device here consists of a circularly focussed 27 finger-pair, 30 μm wavelength (λ) set of 200 nm of aluminium on 7 nm chrome interdigital transducers (IDTs) spanning 25°, where the geometric focal point is 170 μm from the last finger pair, patterned on a 0.5 mm thick 128° *Y*–cut, *X*–propagating lithium niobate ($LiNbO_3$) substrate. The resonant frequency is given by $f = c_s/\lambda$, such that the displacement emanating from one set of finger pairs is reinforced on arrival at a subsequent pair. For $c_s = 3960$ m/s, this condition occurs at $f = 132$ MHz, producing a confined beam approximately 100 μm wide. The PDMS chamber was fabricated on a silicon mould etched using conventional Bosch process deep reactive ion etching (Oxford Instruments PLASMALAB100 ICP380, Abingdon, United Kingdom). The 2 μm thick feature used to produce the membrane results in less influx of etchant ions (SF_6), and therefore a slower etch rate. The result here is that, for a 40 μm deep etch elsewhere, the etch depth within the 2 μm gap is only ≈29 μm, yielding (after soft lithography) a PDMS channel with a height of 40 μm in most locations and a 11 μm gap where the 2 μm feature was patterned. To prevent particle adhesion, a 0.2% w/w solution of polyethylene glycol was flushed through the channels prior to use and used as the makeup volume for particle solutions. Demoulding from the silicon wafer was enhanced by finishing the etching process with a passivation step (C_4F_8) to yield a hydrophobic surface layer. The PDMS was then bonded directly to the SAW device (Harrick Plasma PDC-32G, Ithaca, NY, 1000 mTorr, 18 W), with the influx of polystyrene particles (Magsphere, Pasadena, CA, USA) and DI water modulated by a syringe pump (KDS100, KD Scientific, Holliston, MA, USA). The chamber directly above the IDTs is fully enclosed and air-filled to minimize amplitude attenuation.

Figure 3 shows the capture efficiency for different applied power levels and average flow velocities; higher applied power levels, and therefore larger acoustic pressure amplitudes, result in greater capture efficiency for a given flow rate. Once the SAW is turned off, the incoming particle flow is sufficient to dislodge the captured particles within a few hundred milliseconds. A significant advantage of utilizing both the primarily vertical orientation of the traveling acoustic field and a membrane impeding particle flow is the efficiency of this method; a particle need not be actively forced directly against the direction of particle flow, but in this case only pushed vertically by the distance between the channel floor and the base of the membrane and retained against the smaller local flow velocity. The result is that we are able to efficiently capture and concentrate smaller sized particles (which are acted on by a smaller acoustic force) at lower power levels compared to other SAW-based particle concentration work.[23] In the multimedia for Fig. 3, it is observed that particle motion in the meander region will seem to slow down with the application of SAW. While recent work has demonstrated that the application of SAW can potentially alter the local pressure conditions,[11] it is

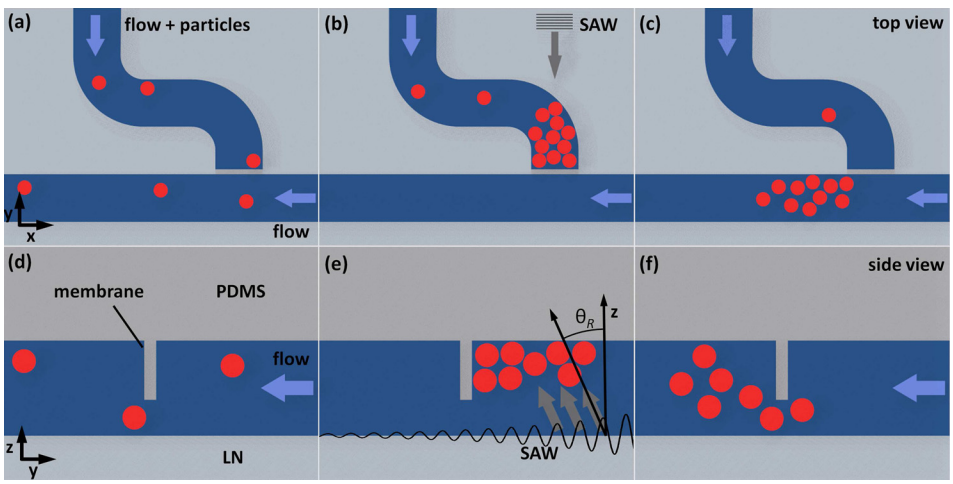

FIG. 2. Diagram of the active process for particle concentration and controlled release in a quasi-3D microfabricated PDMS channel on LN. Without SAW, ((a) and (d)) a continuous dilute stream of particles continues in the direction of fluid flow under the PDMS membrane. (b) and (e) With the application of a SAW generating an acoustic field oriented (primarily vertically) at the Rayleigh angle θ_R, particles are pushed vertically and remain trapped between the membrane and the chamber roof. (c) and (f) With the removal of this pressure source, the now concentrated particles are free to continue in the direction of the flow.

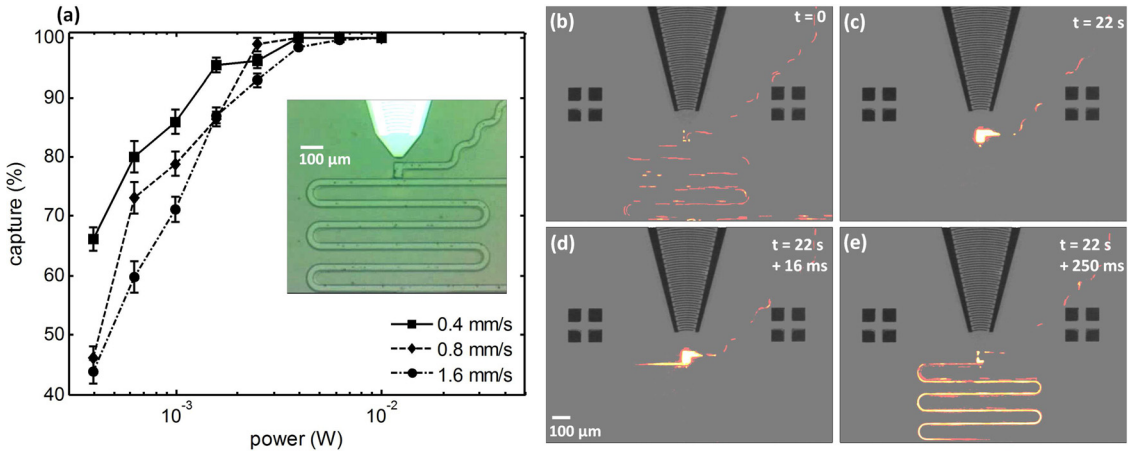

FIG. 3. Experimental results and images of particle concentration and release. (a) The capture efficiency is both power and flow velocity dependent, with lower flow rates and higher powers (with correspondingly higher substrate velocities) resulting in greater capture efficiency. The meander through which the particles flow (inset) is contrast-optimized to show the channel walls, as opposed to the fluorescent images in (b)–(e). (b) Dilute fluorescent 5 μm particles continue unimpeded through a microfluidic meander until the application of SAW. After an arbitrary amount of time, (c) here 22 s, SAW is turned off, leading to ((d) and (e)) near-complete release of the now concentrated particles within a few hundred milliseconds. Images (b)–(e) are with an applied power of 6.2 mW at a flow rate of 1.6 mm/s. Average flow velocities of 0.4 mm/s, 0.8 mm/s, and 1.6 mm/s correspond to flow rates of 0.5 nl/s, 1 nl/s, and 2 nl/s.(Multimedia view) [URL: http://dx.doi.org/10.1063/1.4891424.1]

thought that the change in particle velocity is a result of an acoustic field continuing to propagate into this region pushing particles toward channel edges, rather than as a result of altering fluid velocity. Indeed, the particle outside of this region does not visibly change with the application of SAW.

In the case of a traveling wave, the force applied to a given particle of radius R proportional to R^6 with larger particles therefore subject to a greater time-averaged force.[22] This principle can also be used here to filter and sort particles based on size. When a solution of different particle sizes is subject to the same flow and pressure amplitude conditions, larger particles are preferentially captured behind the PDMS membrane. This is demonstrated in Fig. 4, with 5 μm particles captured and filtered from smaller 2 μm particles. The sorting efficiency here is complete; with sufficient power 100% of the 5 μm are captured and 2 μm particles continuously flowing through the membrane gap. The sorting efficiency (in terms of the proportion of sizes separated) here is comparable to a dedicated traveling SAW separation method,[24] where the SAW is instead oriented orthogonally to the flow direction. However, as the separation ability here is supplementary to the main function of controlled capture and release, separation is limited to instances where, in a population of two distinct particle sizes, only one particle size is significantly influenced by the acoustic force field (with amplitude F_{aco}), while the other's motion is dominated by a viscous drag force F_D. In the case of a population of 2 μm and 5 μm particles, this condition is satisfied, where the 5 μm particles are subject to a F_{aco}/F_D two orders of magnitude greater than that of the 2 μm ones. However, where the particle sizes are more similar, as in the case of a 5/7 μm population, no effective sorting is observed. This is partly due to the varying local viscous drag in the vicinity of the membrane, which is almost zero in the corner near the channel ceiling and at a maximum near the gap between the membrane and the channel floor; a more efficient sorting mechanism would attempt to equalize the local fluid velocity as well as acoustic pressure amplitude experience by all particles as in Ref. 16. Sorting efficiency is also reduced as the particle size approaches that of the wavelength in the fluid ($\approx$11 μm at 132 MHz in water), where the acoustic force scaling is reduced (from R^6 to R^2).[22,25,26] In general, acoustic sorting efficiency is optimized by choosing a

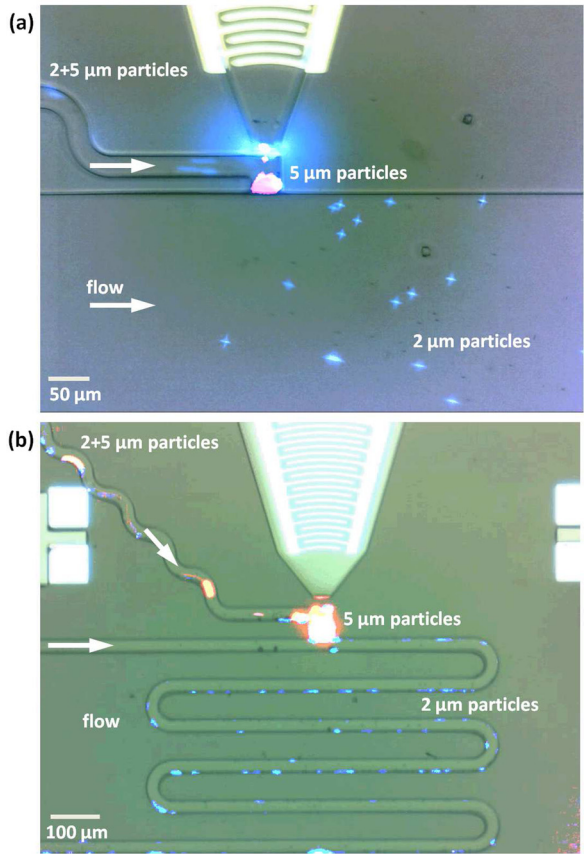

FIG. 4. Experimental images of particle filtering, here with 4 mW of applied power and a particle input flow rate of $\approx$1 mm/s, showing a superimposed optical fluorescent image of 5 μm (red) and 2 μm (blue) particles for both (a) a wide aspect ratio chamber and the same channel from Fig. 3. The larger particles, subject to a greater acoustic force, are wedged preferentially at the corner of the chamber roof and membrane, allowing the smaller 2 μm particles to pass under the membrane into the open chamber unimpeded.

sufficiently high frequency for a given particle population so the increase in force with frequency can be taken advantage of—recent work has demonstrated the significant deflection of 2 μm particles at higher frequencies, something that was not observed here[13]—but not so high that the resulting acoustic wavelength approaches the size of the particle and the differential acoustic force between particle sizes is reduced.

Here, we have demonstrated a SAW-based controlled capture and release mechanism with potential application to a range of microfluidic systems. The low power nature of this method, requiring only milliwatts—on the order of that used in portable RF communication devices—makes it readily applicable to handheld, point of care diagnostic devices. Furthermore, the scale of the SAW device demonstrated here, with an aperture of only 100 μm and totaling less than a millimeter in length, is of the small size needed to be integrated into these systems. Future work in SAW microfluidic lab-on-a-chip systems, moving from the conceptual and demonstration phase, will need to move increasingly in the direction of miniaturization such as that demonstrated here.

We gratefully acknowledge support received from the Australian Research Council, Grant No. DP 110104010. This work was performed in part at the Melbourne Centre for Nanofabrication (MCN) in the Victorian Node of the Australian National Fabrication Facility (ANFF).

[1]F. Beyeler, A. Neild, S. Oberti, D. J. Bell, Y. Sun, J. Dual, and B. J. Nelson, J. Microelectromech. Syst. **16**, 7 (2007).
[2]A. Neild, S. Oberti, F. Beyeler, J. Dual, and B. J. Nelson, J. Micromech. Microeng. **16**, 1562 (2006).
[3]A. H. Yang, S. D. Moore, B. S. Schmidt, M. Klug, M. Lipson, and D. Erickson, Nature **457**, 71 (2009).
[4]D. G. Grier, Nature **424**, 810 (2003).
[5]P. J. Lee, P. J. Hung, R. Shaw, L. Jan, and L. P. Lee, Appl. Phys. Lett. **86**, 223902 (2005).
[6]E. Mirowski, J. Moreland, S. Russek, M. Donahue, and K. Hsieh, J. Magn. Magn. Mater. **311**, 401 (2007).
[7]E. Mirowski, J. Moreland, A. Zhang, S. E. Russek, and M. J. Donahue, Appl. Phys. Lett. **86**, 243901 (2005).
[8]D. Collins, T. Alan, K. Helmerson, and A. Neild, Lab Chip **13**, 3225 (2013).
[9]P. Rogers and A. Neild, Lab Chip **11**, 3710 (2011).
[10]S. Oberti, D. Moeller, A. Neild, J. Dual, F. Beyeler, B. Nelson, and S. Gutmann, Ultrasonics **50**, 247 (2010).
[11]L. Schmid and T. Franke, Appl. Phys. Lett. **104**, 133501 (2014).
[12]J. Shi, H. Huang, Z. Stratton, Y. Huang, and T. J. Huang, Lab Chip **9**, 3354 (2009).
[13]V. Skowronek, R. W. Rambach, L. Schmid, K. Haase, and T. Franke, Anal. Chem. **85**, 9955 (2013).
[14]L. Schmid, D. A. Weitz, and T. Franke, "Sorting drops and cells with acoustics: acoustic microfluidic fluorescence-activated cell sorter," Lab Chip (published online).
[15]L. Johansson, J. Enlund, S. Johansson, I. Katardjiev, and V. Yantchev, Biomed. Microdevices **14**, 279 (2012).
[16]D. J. Collins, T. Alan, and A. Neild, Lab Chip **14**, 1595 (2014).
[17]O. Manor, L. Y. Yeo, and J. R. Friend, J. Fluid Mech. **707**, 482 (2012).
[18]M. B. Dentry, J. R. Friend, and L. Y. Yeo, Lab Chip **14**, 750 (2014).
[19]J. Rooney and W. Nyborg, Am. J. Phys. **40**, 1825 (1972).
[20]H. Bruus, Lab Chip **12**, 1014 (2012).
[21]D. Baresch, J.-L. Thomas, and R. Marchiano, J. Acoust. Soc. Am. **133**, 25 (2013).
[22]L. V. King, Proc. R. Soc. London, Ser. A **147**, 212 (1934).
[23]Y. Chen, S. Li, Y. Gu, P. Li, X. Ding, L. Wang, J. P. McCoy, S. J. Levine, and T. J. Huang, Lab Chip **14**, 924 (2014).
[24]G. Destgeer, K. H. Lee, J. H. Jung, A. Alazzam, and H. J. Sung, Lab Chip **13**, 4210 (2013).
[25]T. Hasegawa and K. Yosioka, J. Acoust. Soc. Am. **58**, 581 (1975).
[26]T. Hasegawa and K. Yosioka, J. Acoust. Soc. Am. **46**, 1139 (1969).